

Magnetotransport and thermoelectricity in disordered graphene

Balázs Dóra*

Max-Planck-Institut für Physik Komplexer Systeme, Nöthnitzer Str. 38, 01187 Dresden, Germany

Peter Thalmeier

Max-Planck-Institut für Chemische Physik fester Stoffe, 01187 Dresden, Germany

(Dated: October 10, 2018)

We have studied the electric and thermal response of two-dimensional Dirac-fermions in a quantizing magnetic field in the presence of localized disorder. The electric and heat current operators in the presence of magnetic field are derived. The self-energy due to impurities is calculated self-consistently, and depends strongly on the frequency and field strength, resulting in asymmetric peaks in the density of states at the Landau level energies, and small islands connecting them. The Shubnikov-de Haas oscillations remain periodic in $1/B$, in spite of the distinct quantization of quasiparticle orbits compared to normal metals. The Seebeck coefficient depends strongly on the field strength and orientation. For finite field and chemical potential, the Wiedemann-Franz law can be violated.

PACS numbers: 81.05.Uw,71.10.-w,73.43.Qt

I. INTRODUCTION

Recent advances of nanotechnology have made the creation and investigation of two dimensional carbon, called graphene, possible^{1,2,3,4}. It is a monolayer of carbon atoms packed densely in a honeycomb structure. In spite of being few atom thick, these systems were found to be stable and ready for exploration. One of the most intriguing property of graphene is, that its charge carriers are well described by the relativistic Dirac's equation, and are two-dimensional Dirac fermions⁵. This opens the possibility of investigating "relativistic" phenomena at a speed of $\sim 10^6$ m/s (the Fermi velocity of graphene), 1/300th the speed of light. The linear, Dirac-like spectrum causes the density of states to increase linearly with energy, which is to be contrasted the constant density of states of normal metals. Due to this peculiar property, the response of graphene to external probes is expected to be unusual. This manifests itself in the anomalous integer quantum Hall effect⁶, which occurs at half-integer filling factors, and in the presence of universal minimal value of the conductance. The dependence of the thermal conductivity on applied magnetic field has been measured in highly oriented pyrolytic graphite^{7,8}.

Dirac-fermions show up in other systems, at least from the theoretical side. They characterize the low energy properties of orbital antiferromagnets, a density wave system with a gap of d-wave symmetry^{9,10}. A similar model has been proposed for the pseudogap phase of high T_c cuprate superconductors, known as d-density wave, with peculiar electronic properties¹¹. A similar system was also mentioned in the context of heavy fermion material URu₂Si₂, which shows a clear phase transition at 17 K without any obvious long range order, detectable by X-ray or NMR experiments. Its low temperature phase was attributed to another spin density wave with a d-wave gap^{12,13}. Experimentally, the aforementioned materials possess unusual electric and thermal responses as a function of temperature and magnetic field^{14,15}.

Therefore, the interest in studying the transport properties of two-dimensional Dirac-fermions is not surprising. Gusynin, Sharapov and coworkers have studied exhaustively^{16,17,18,19,20,21,22} the electric and thermal response of two-dimensional systems with linear energy spectrum, with special emphasis on the Wiedemann-Franz law and magnetic oscillations. However, their self energy due to scattering from impurities was not determined in a self-consistent manner, but rather they assumed a constant, energy, magnetic field and temperature independent scattering rate. Moreover, they completely neglected the real part of the self energy, responsible for the shift of energy levels. Nevertheless, they derived beautiful analytical formulas for the various transport coefficients, which, although suffering from the above limitations, turned out to be useful in explaining experiments⁶.

Impurity scattering can be taken into account in the presence of quantizing magnetic field in the usual self-consistent way²³. This program has been carried out, among many others²⁴, by Peres et al.²⁵. In their work, the full self-consistent Born approximation was used before taking the strength of the impurity potential to infinity. They studied the frequency dependence of the electric conductivity for various fields, but never entered into the realm of thermal transport. Parallel studies have also been performed in the limit of weak-scatterers^{26,27}.

In this paper, we extend the work of Refs. 16,17,18,19, and determine self-consistently the energy and magnetic field dependent self-energies and study the Seebeck coefficient as well, and also generalize Ref. 25 to include thermoelectricity. We study Dirac-fermions in a Landau quantizing magnetic field (B) in the presence of scatterers, allowing for arbitrary field orientations. In a way, our study here bridges between the efforts of the previous groups. After

the introduction of the general formalism, we determine the electric and heat current operators, essential for further steps. By introducing impurities in the system, we can study the quasiparticle density of states, the electric and heat conductivity, the Seebeck coefficient and the Wiedemann-Franz law as a function of magnetic field strength and orientation and temperature. For high fields, the discrete nature of the Landau levels is revealed in the density of states in the form of asymmetric peaks at Landau level energies (far from being Lorentzians), which smoothen with decreasing field. Shubnikov-de Haas oscillation are visible in all transport coefficients, periodic in $1/B$, similarly to normal metals²⁸. The angular dependent conductivity oscillations become more pronounced with increasing field. The chemical potential dependence of the conductivity resembles closely the experimental findings⁶. The Seebeck coefficient depends strongly on the applied field and temperature.

II. LANDAU QUANTIZATION, ELECTRIC AND HEAT CURRENT

The Hamiltonian of non-interacting quasiparticles living on a single graphene sheet is given by^{25,29,30}:

$$H_0 = -v_F \sum_{j=x,y} \sigma_j (-i\partial_j + eA_j(\mathbf{r})), \quad (1)$$

where σ_j 's are the Pauli matrices, and stand for Bloch states residing on the two different sublattices of the bipartite hexagonal lattice of graphene^{18,25}. Strictly speaking, the Hamiltonian above describes quasiparticles around the K points of the Brillouin zone, where the spectrum vanishes. The vector potential for a constant, arbitrarily oriented magnetic field reads as $\mathbf{A}(\mathbf{r}) = (-By \cos \theta, 0, B(y \sin \theta \cos \phi - x \sin \theta \sin \phi))$, where θ is the angle the magnetic field makes from the z axis, and ϕ is the in-plane polar-angle measured from the x -axis. We have dropped the Zeeman term, its energy would be negligible with respect to energy of the Landau levels, Eq. (5), using $v_F \approx 10^6$ m/s, characteristic to graphene. Eq. (1) applies for both spin directions.

In the absence of magnetic field, the energy spectrum of the system is given by

$$E(\mathbf{k}) = \pm v_F |\mathbf{k}|. \quad (2)$$

This describes massless relativistic fermions with spectrum consisting of two cones, touching each other at the end-points. From this, the density of states per spin follows as

$$\rho(\omega) = \frac{1}{\pi} \sum_{\mathbf{k}} \delta(\omega - E(\mathbf{k})) = \frac{1}{\pi} \frac{A_c}{2\pi} \int_0^{k_c} k dk \delta(\omega \pm v_F k) = \frac{2|\omega|}{D^2}, \quad (3)$$

where k_c is the cutoff, $D = v_F k_c$ is the bandwidth, and $A_c = 4\pi/k_c^2$ is the area of the hexagonal unit cell.

In the presence of magnetic field, the eigenvalue problem of this Hamiltonian ($H_0\Psi = E\Psi$) can readily be solved²⁵. For the zero energy mode ($E=0$), the eigenfunction is obtained as

$$\Psi_k(\mathbf{r}) = \frac{e^{ikx}}{\sqrt{L}} \begin{pmatrix} 0 \\ \phi_0(y) \end{pmatrix}, \quad (4)$$

and the two components of the spinor describe the two bands. The energy of the other modes read as

$$E(n, \alpha) = \alpha \omega_c \sqrt{n+1} \quad (5)$$

with $\alpha = \pm 1$, $\omega_c = v_F \sqrt{2e|B \cos(\theta)|}$ is the cyclotron frequency, $n = 0, 1, 2, \dots$. Only the perpendicular component of the field enters into these expressions, and by tilting the field away from the perpendicular direction corresponds to a smaller effective field. The sum over integer n 's is cut off at N given by $N+1 = (D/\omega_c)^2$, which means that we consider $2N+3$ Landau levels altogether. For later convenience, we define a magnetic field B_0 , whose cyclotron frequency is equal to the bandwidth ($\omega_c = D$).

The corresponding wave function is

$$\Psi_{n,k,\alpha}(\mathbf{r}) = \frac{e^{ikx}}{\sqrt{L}} \begin{pmatrix} \phi_n(y - kl_B^2) \\ \alpha \phi_{n+1}(y - kl_B^2) \end{pmatrix} \quad (6)$$

with cyclotron length $l_b = 1/\sqrt{eB}$. Here $\phi_n(x)$ is the n th eigenfunction of the usual one-dimensional harmonic oscillator. The electron-field operator can be built up from these functions as

$$\Psi(\mathbf{r}) = \sum_k \left[\Psi_k(\mathbf{r}) c_k + \sum_{n,\alpha} \Psi_{n,k,\alpha} c_{k,n,\alpha} \right]. \quad (7)$$

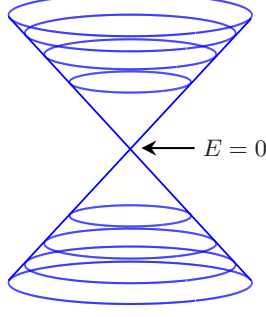


FIG. 1: The structure of the Landau levels is visualized schematically for the first few levels.

The Green's functions of these new operators do not depend on k , and read as

$$G_0(i\omega_n, k) = \frac{1}{i\omega_n}, \quad (8)$$

$$G_0(i\omega_n, k, n, \alpha) = \frac{1}{i\omega_n - E(n, \alpha)} \quad (9)$$

for c_k and $c_{k,n,\alpha}$, respectively, and ω_n is the fermionic Matsubara frequency.

With the use of these, we can determine the electric and heat current operators of the system. Following Mahan³¹, we define the polarization operator as

$$\mathbf{P} = \frac{1}{2} \int d\mathbf{r} (\mathbf{r}\rho(\mathbf{r}) + \rho(\mathbf{r})\mathbf{r}) \quad (10)$$

with $\rho(\mathbf{r}) = \Psi^\dagger(\mathbf{r})\Psi(\mathbf{r})$ giving the charge density, and the symmetric combination ensures hermiticity. The total current is its time derivative, which follows as

$$\mathbf{J} = \partial_t \mathbf{P} = i[H, \mathbf{P}]. \quad (11)$$

By performing the necessary steps, after straightforward calculations this yields²⁵

$$J_x = v_F e \sum_{p,\alpha} \left[\frac{1}{\sqrt{2}} (c_p^\dagger c_{p,0,\alpha} + c_{p,0,\alpha}^\dagger c_p) + \sum_{n,\lambda} \frac{\lambda}{2} (c_{p,n+1,\alpha}^\dagger c_{p,n,\lambda} + c_{p,n,\lambda}^\dagger c_{p,n+1,\alpha}) \right], \quad (12)$$

$$J_y = iv_F e \sum_{p,\alpha} \left[\frac{1}{\sqrt{2}} (c_p^\dagger c_{p,0,\alpha} - c_{p,0,\alpha}^\dagger c_p) + \sum_{n,\lambda} \frac{\lambda}{2} (c_{p,n,\lambda}^\dagger c_{p,n+1,\alpha} - c_{p,n+1,\alpha}^\dagger c_{p,n,\lambda}) \right]. \quad (13)$$

The heat current operator for the pure system can be determined similarly. In analogy with polarization, one defines the energy position operator³² as

$$\mathbf{R}^E = \frac{1}{2} \int d\mathbf{r} (\mathbf{r}H(\mathbf{r}) + H(\mathbf{r})\mathbf{r}), \quad (14)$$

and the total Hamiltonian is $H = \int d\mathbf{r} H(\mathbf{r})$. Using this, one deduces the energy current from

$$\mathbf{J}^E = \partial_t \mathbf{R}^E. \quad (15)$$

This leads to

$$J_x^E = \frac{v_F e}{2} \sum_{p,\alpha} \left[\frac{E(0, \alpha)}{\sqrt{2}} (c_p^\dagger c_{p,0,\alpha} + c_{p,0,\alpha}^\dagger c_p) + \sum_{n,\lambda} \frac{\lambda}{2} (E(n+1, \alpha) + E(n, \lambda)) (c_{p,n+1,\alpha}^\dagger c_{p,n,\lambda} + c_{p,n,\lambda}^\dagger c_{p,n+1,\alpha}) \right], \quad (16)$$

$$J_y^E = \frac{iv_F e}{2} \sum_{p,\alpha} \left[\frac{E(0, \alpha)}{\sqrt{2}} (c_p^\dagger c_{p,0,\alpha} - c_{p,0,\alpha}^\dagger c_p) + \sum_{n,\lambda} \frac{\lambda}{2} (E(n+1, \alpha) + E(n, \lambda)) (c_{p,n,\lambda}^\dagger c_{p,n+1,\alpha} - c_{p,n+1,\alpha}^\dagger c_{p,n,\lambda}) \right]. \quad (17)$$

These follow naturally from the electric current operator, after multiplying each term with the corresponding mode energy. Note, that the energy of the state labeled solely by (p) is zero, it belongs to the state situated at the meeting point of the two cones. Finally the heat current operator is related to the energy current by the simple formula: $\mathbf{J}^Q = \mathbf{J}^E - \mu\mathbf{J}$, μ is the chemical potential. So far we have considered the particle-hole symmetric case with $\mu = 0$, but we can easily use a finite chemical potential to break this symmetry, and introduce finite Seebeck coefficient.

III. IMPURITY SCATTERING IN THE PRESENCE OF MAGNETIC FIELD

In the presence of impurities, an extra term is added to the Hamiltonian:

$$H_{imp} = V \sum_{i=1}^{N_i} \delta(\mathbf{r} - \mathbf{r}_i). \quad (18)$$

As a result, the explicit form of the previous operators might change. However, using Eq. (18), the electric current remains unchanged, but the heat current changes due to the non-commutativity of the impurity Hamiltonian and the energy position operator³¹. As a result, impurities need to be taken into account not only in the calculation of the self-energy, but also in the form of the operators, and one has to use the same level of approximation for both.

However, to avoid this difficulty, one can replace the energy terms in \mathbf{J}^E by the Matsubara frequency³², since from the poles of the Green's function, this will pick the appropriate energy. This replacement works perfectly in the case of impurities as well, when quasiparticle excitations possess finite lifetime.

Since graphene is two-dimensional, positional long range order (i.e. lattice formation) is impossible at finite temperatures, since thermal fluctuations will destroy it. This is why the introduction of defect is natural in this system. To mimic disorder, we have chosen to spread vacancies in the honeycomb lattice, which can be modeled by taking the impurity strength (V) to infinity.

To take scattering into account, we have to determine the explicit form of H_{imp} in the Landau basis. Then the standard non-crossing approximation can be used²³, which, in the case of graphene, is called the full self-consistent Born approximation due to the neglect of crossing diagrams^{25,26,27}. Averaging over impurity positions is performed in the standard way. By letting the impurity strength $V \rightarrow \infty$, which would correspond to the unitary scattering limit in unconventional superconductors³³, we arrive to the following set of equations²⁵:

$$G(i\omega_n, k, n, \alpha) = \frac{1}{i\omega_n - E(n, \alpha) - \Sigma_1(i\omega_n)}, \quad (19)$$

$$G(i\omega_n, k) = \frac{1}{i\omega_n - \Sigma_2(i\omega_n)}, \quad (20)$$

where

$$\Sigma_1(i\omega_n) = -\frac{2n_i}{g_c[G(i\omega_n, k) + \sum_{n, \alpha} G(i\omega_n, k, n, \alpha)]}, \quad (21)$$

$$\Sigma_2(i\omega_n) = -\frac{2n_i}{g_c[2G(i\omega_n, k) + \sum_{n, \alpha} G(i\omega_n, k, n, \alpha)]}, \quad (22)$$

where $g_c = 1/(N + 1)$ is the degeneracy of a Landau level per unit cell, n_i is the impurity concentration. The summation over Landau levels can be performed to yield

$$\sum_{n, \alpha} G(i\omega_n, k, n, \alpha) = 2\frac{z}{\omega_c} \{ \Psi(1 - z^2) - \Psi(N + 2 - z^2) \}, \quad (23)$$

where $z = (i\omega_n - \Sigma_1(i\omega_n))/\omega_c$, $\Psi(z)$ is the digamma function. The self-consistency equations can further be simplified, and after analytic continuation to real frequencies ($i\omega_n \rightarrow \omega + i0^+$), we can read off

$$\Sigma_1(\omega) = \Sigma_2(\omega) \frac{2n_i(\omega - \Sigma_2(\omega))}{g_c \Sigma_2(\omega) + 2n_i(\omega - \Sigma_2(\omega))}. \quad (24)$$

At zero frequency, this simplifies to

$$\Sigma_2(0) = \Sigma_1(0) \left(1 - \frac{1}{2n_i(N + 1)} \right). \quad (25)$$

The imaginary part of the self energy is always negative to ensure causality. This means that the last term in parenthesis on the right hand side must always be positive to assure the same sign of the imaginary parts of the self energies. This translates into

$$n_i \geq \frac{1}{2(N+1)}. \quad (26)$$

For each impurity concentration, there is a certain magnetic field strength (when $N = (1/2n_i) - 1$), above which our approximation breaks down. For higher field, the self energy at zero frequency needs to be zero to fulfill Eq. (25) and causality. This means, that at a finite impurity concentration, we still have excitations in the system with infinite lifetime. Further, we are going to show that this occurs not only on the zeroth Landau level, but on all Landau levels for field exceeding the critical one. To improve on this, crossing diagrams need to be considered, which is beyond the scope of the present work. Hence we restrict our investigation to fields allowed by Eq. (26). The larger the impurity concentration, the larger the magnetic field we can take into account.

The quasiparticle density of states can be evaluated from the knowledge of the Green's function, and it reads as

$$\rho(\omega) = \frac{2n_i}{\pi} \text{Im} \frac{1}{\Sigma_1(\omega)}. \quad (27)$$

Without impurities, the density of states consists of Dirac-delta peaks located at zero frequency and at $E(n, \alpha)$. By introducing impurities in the system, we expect the broadening and shift of these levels, and it can be determined from the solution of the self consistency equations.

For large magnetic fields (small N), we can still solve the self-consistency equations Eqs. (21)-(22), but we discover Dirac-delta peaks at the position of the levels and small islands between them (Fig. 2, $N = 100$). This signals that the non-crossing approximation is insufficient to provide these peaks with a finite broadening. As we decrease the field (increase N), the peaks and islands merge, and all excitations possess finite lifetime, but clean gaps are still observable between the levels. By further decreasing the field, the gaps disappear, the density of states becomes finite for all energies, and small successive bumps remain present due to Landau level formation, which tend to be smoothed by further decreasing the field. In this limit, the resulting density of states is very close to that in a d-wave superconductor³⁴, stemming from its linear frequency dependence in the pure case.

The broadening of the levels is not symmetric, more spectral weight is transferred to the lower energy part, which arises from the important energy dependence of the imaginary part of the self energies. Also the level position is modified in the presence of impurities due to the finite real part of the self energies, and this shift increases with the impurity concentration.

The numerical solution of Eqs. (21)-(22), and the resulting density of states is shown in Fig. 2. From this, one can conjecture, that a given n_i and N can qualitatively well describe different fields and concentrations, if their product ($n_i N$) is the same. These features, including the non-Lorentzian broadening of the Landau levels and the development of small islands between the levels should be observable experimentally by scanning tunneling microscopy, for example.

IV. ELECTRIC AND THERMAL CONDUCTIVITIES

Using the spectral representation of the Green's functions, we can evaluate the corresponding conductivities after straightforward but lengthy calculations. These are related to the time ordered products of the form³¹

$$\Pi_{i,j}^{AB}(i\omega) = - \int_0^\beta d\tau e^{i\omega\tau} \langle T_\tau J_i^A(\tau) J_j^B(0) \rangle, \quad (28)$$

where A and B denote the electric or heat current, i and j stand for the spatial component. These can be expressed with the use of the following transport integrals²⁸:

$$L_n = \int_{-\infty}^{\infty} \frac{d\epsilon}{4T} \frac{\sigma(\epsilon)}{\cosh^2((\epsilon - \mu)/2T)} \left(\frac{\epsilon - \mu}{T} \right)^n, \quad (29)$$

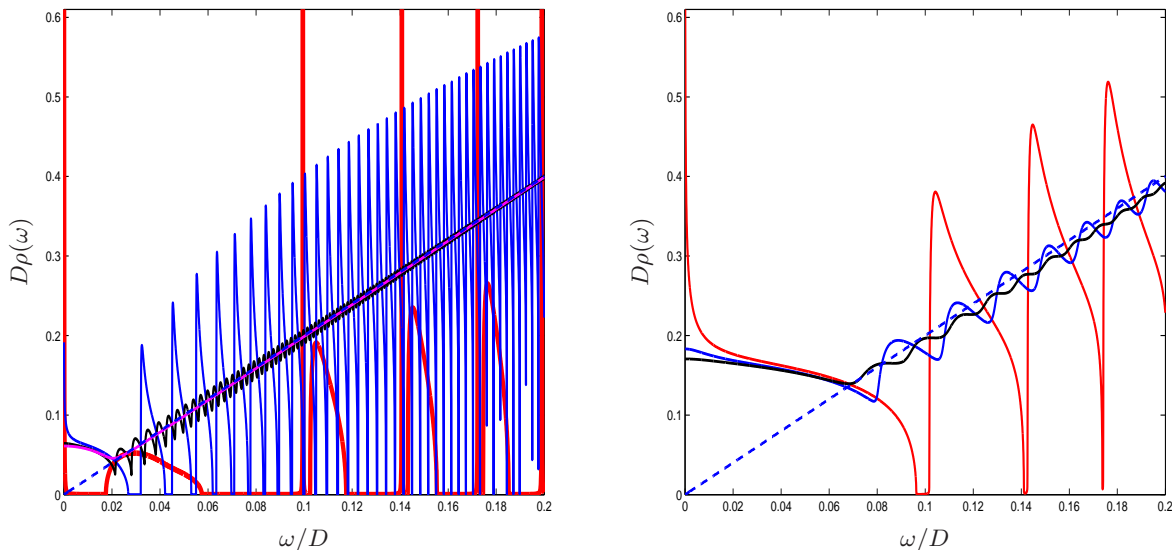


FIG. 2: (Color online) The density of states is shown in the left panel for $n_i = 0.001$ for $N = 100$ (red), 1000 (blue), 3000 (black), 10000 (magenta). The vertical red lines stand for the Dirac-delta peaks for $N = 100$. The right panel visualizes the $n_i = 0.01$ case for $N = 100$ (red), 200 (blue), 300 (black). The clean case without magnetic field ($N = \infty$) is also plotted for comparison in both panels (blue dashed line).

where

$$\sigma(\epsilon) = \omega_c^2 \sum_{\alpha} \left[\frac{\text{Im}\Sigma_2(\epsilon)}{(x - \text{Re}\Sigma_2(\epsilon))^2 + (\text{Im}\Sigma_2(\epsilon))^2} \frac{\text{Im}\Sigma_1(\epsilon)}{(x - E(0, \alpha) - \text{Re}\Sigma_1(\epsilon))^2 + (\text{Im}\Sigma_1(\epsilon))^2} + \right. \\ \left. + \frac{1}{2} \sum_{n, \lambda} \frac{\text{Im}\Sigma_1(\epsilon)}{(x - E(n, \alpha) - \text{Re}\Sigma_1(\epsilon))^2 + (\text{Im}\Sigma_1(\epsilon))^2} \frac{\text{Im}\Sigma_1(\epsilon)}{(x - E(n+1, \lambda) - \text{Re}\Sigma_1(\epsilon))^2 + (\text{Im}\Sigma_1(\epsilon))^2} \right] \quad (30)$$

is the dimensionless conductivity kernel. With the use of these, we obtain the various transport coefficients as usual:

$$\sigma = \frac{2e^2}{\pi h} L_0, \quad (31)$$

$$S = \frac{1}{e} \frac{L_1}{L_0}, \quad (32)$$

$$\frac{\kappa}{T} = \frac{2}{\pi h} \left(L_2 - \frac{L_1^2}{L_0} \right), \quad (33)$$

$$L = \frac{\kappa}{\sigma T} = \frac{1}{e^2} \frac{L_2 L_0 - L_1^2}{L_0^2}. \quad (34)$$

Here, σ is the electric conductivity, S is the Seebeck coefficient, κ is the heat conductivity, where the last term ensures that the energy current is evaluated under the condition of vanishing electric current, and L is the Lorentz number. Off diagonal components of the conductivity tensors, such as the Nernst coefficient, are also of prime interest, but they cannot be simply evaluated from Kubo formula. Even in the case of a normal metal with parabolic dispersion, the Kubo formula turned out to be invalid^{35,36}, and additional corrections have been worked out. Their determination for two-dimensional Dirac fermions is beyond the scope of the present investigation.

For the particle-hole symmetric case ($\mu = 0$), the Seebeck coefficient is trivially zero. If we consider the zero temperature, half-filled case, and assume small magnetic fields, we obtain the universal conductivity given by

$$\sigma_0 = \frac{2e^2}{\pi h}, \quad (35)$$

and similarly for the thermal conductivity as

$$\frac{\kappa}{T} = \frac{2e^2 \pi}{3h}. \quad (36)$$

The Seebeck coefficient is zero. From this, the Lorentz number takes its universal value

$$L_u = \frac{\pi^2}{3} \left(\frac{k_B}{e} \right)^2, \quad (37)$$

which means, that in this limit, the Wiedemann-Franz law holds^{16,23}. Landau levels always develop around the meeting point of the conical valence and conduction band. If we are at half filling ($\mu = 0$), no levels cross μ when varying the magnetic field, since they are symmetrically placed below and above. However, when μ is finite, Landau levels can cross its value with changing the field, and we expect Shubnikov-de Haas oscillations. In general, when the number of levels below μ is large (or $\omega_c \ll |\mu|$), we can conjecture the periodicity of these oscillations. Assume that a level (the n th) sits right at the chemical potential ($\mu = \omega_c \sqrt{n+1}$). Then, the distance from the adjacent level determines the period of the oscillations. This is

$$|E(n+1, \alpha) - E(n, \alpha)| \approx \frac{\omega_c}{2\sqrt{n+1}} = \frac{\omega_c^2}{2\mu} = \frac{v_F^2 e |B \cos(\theta)|}{\mu} \sim B \quad (38)$$

provided, that $n \gg 1$. This means, that albeit the Landau levels show an unusual $\propto \sqrt{n}$ dependence of the level index compared to that in a normal metal $\propto n$, the Shubnikov-de Haas oscillations turn out to be still periodic as a function of $1/B$. The comparison of the coefficient of the magnetic field in Eq. (38) to that in a parabolic band²⁸ suggests, that the cyclotron mass can be defined as $m_c = \mu/v_F^2$. Even though the spectrum is linear, the finite chemical potential provides us with an energy scale for m_c ⁶. This can readily be checked in Fig. 3, where not only the field, but the angle dependence of the conductivity is shown for different field strength. The larger the magnetic field, the more visible the oscillations are, although these can be smeared by increasing the concentrations.

The explicit value of the chemical potential, which is fixed by the particle number at a given temperature and field, should also be determined self-consistently. However, no serious deviations from its initial values have been detected during the evaluation process, and these did not affect the dependence of physical quantities on T and B in the investigated range of parameters. Presumably, taking a large value of the chemical potential would require its self-consistent determination as well.

In Fig. 4, we show the magnetic field dependence of the heat conductivity. It resembles closely to the electric one at low temperatures. However, at higher temperatures, each peak in the oscillations split into two. This occurs, because in the electric conductivity, the kernel is sampled by the $1/\cosh^2((\epsilon - \mu)/2T)$ function, which gathers information about excitations at the chemical potential. However, an extra $(\epsilon - \mu)^2$ factor appears in the heat response, which measures the immediate vicinity of μ above and below, within a window $2T$, which gives the splitting. The oscillations become smoothed with decreasing field, in contrast to Ref. 18, where large oscillations were found even at small fields. The difference can be traced back to our field dependent scattering rate (Eqs. (21)-(22)), as opposed to the field independent one used in Ref. 18. Similar features have been observed in highly oriented pyrolytic graphite^{7,8}. By decreasing the field, N increases, and the density of states becomes similar to that of a d-wave superconductor³⁴, without significant deviations from linearity. Both σ and κ decrease with field, a feature already present at $\mu = 0$. As we increase the field, ω_c increases, and so does the distance between Landau levels. Then, at a given temperature, a smaller number of states will be present for excitations around μ , hence the corresponding conductivity decreases. The Seebeck coefficient shows sharp oscillations which die out with temperature. Its background value, after subtracting the oscillations, is found to be almost magnetic field independent, but smoothly increases with temperature. The Lorentz number remains close to one, if we subtract the oscillations. However, due to the double (single) peak structures in the heat (electric) response, their ratio shows wild, but sharp deviations from unity at specific fields, where the Wiedemann-Franz law is violated. In contrast to this, one would have encountered large and wide oscillations in the Lorentz number as a function of field in the presence of phenomenological, constant scattering rate.

In Fig. 5, we show the evolution of the electric and heat conductivity and the Seebeck coefficient as a function of chemical potential. In accordance with experiment in Ref. 6, we also find oscillations, corresponding to Landau levels, which also smoothen with temperature. Interestingly, the splitting of the peaks in the heat conductivity is nicely observable as a function of μ . These occur in such a way that they produce antiphase oscillations with respect to the electric one, and lead to the violation of the Wiedemann-Franz law. The Seebeck coefficient shows peculiar behaviour. At the particle-hole symmetric case, it is zero, and remains mainly so apart from large oscillations.

The temperature dependence of the electric and heat response is shown in Fig. 6. Both increase steadily with temperature, since more available states are accessible with T . However, at small temperatures, a small decrease is observable in low fields, in accordance with other studies^{16,25}. The Seebeck coefficient first increases, and after a broad bump, decreases with T . For higher temperatures, the bandwidth D makes its presence felt. The Wiedemann-Franz law remains intact at low temperatures and fields, but becomes violated for higher T or B .

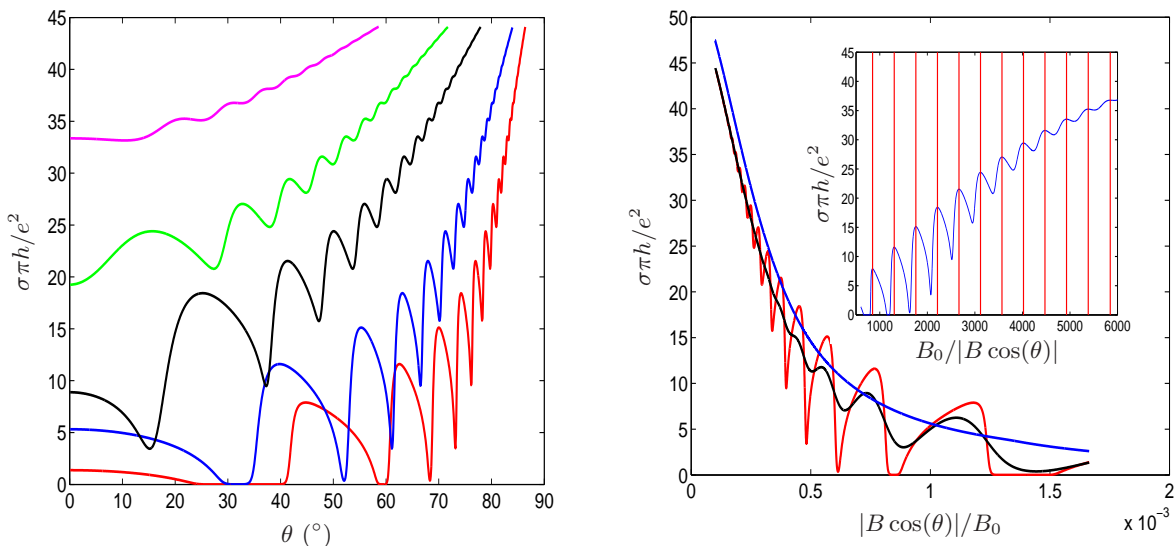


FIG. 3: (Color online) The angular dependent magnetoconductivity oscillations are visualized for $\mu = 0.05D$, $n_i=0.001$ and $T = 0.0001D$, for magnetic fields $N = 600$ (red), 1000 (blue), (2000) (black), (3000) (green) and 5000 (magenta) in the left panel. With increasing field (decreasing N), the oscillations become more pronounced, signaling the discrete Landau level structure. The right panel shows the electric conductivity for $\mu = 0.05D$, $n_i=0.001$ and $T/D = 0.0001$ (red), 0.001 (black) and 0.01 (blue). For higher field, we arrive to the region, where crossing diagrams need to be taken into account. The inset shows the electric conductivity as a function of $1/|B \cos(\theta)|$ to emphasize its periodicity.

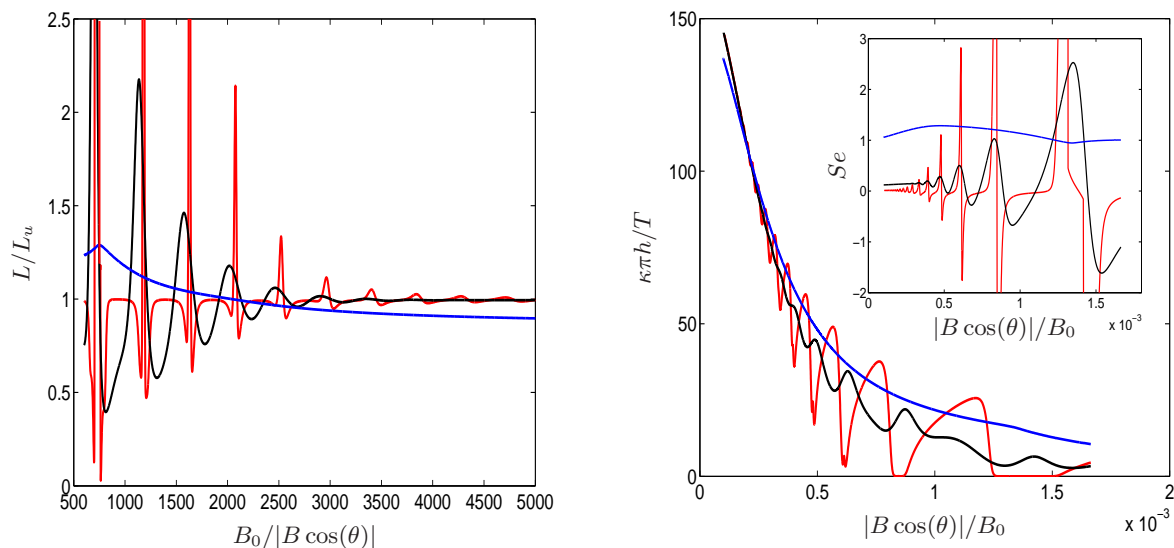


FIG. 4: (Color online) The left panel shows the Lorentz number as a function of the inverse magnetic field to stress the periodic violation of the Wiedemann-Franz law for $\mu = 0.05D$, $n_i=0.001$ and $T/D = 0.0001$ (red), 0.001 (black) and 0.01 (blue). The right panel shows the heat conductivity and the Seebeck coefficient (inset) for the set of same parameters.

V. CONCLUSION

We have studied the effect of localized impurities in two dimensional Dirac fermions in the presence of quantizing, arbitrarily oriented magnetic field. The energy spectrum depends on the level index as $\propto \sqrt{n}$, as opposed to the $n + 1/2$ linear dependence in normal metals²³. Expressions for both the electric and heat current in the presence of magnetic field were worked out. The self-energy in the full Born-approximation obeys self-consistency conditions, resulting in important magnetic field and frequency dependence of scattering rate and level shift. In the density of states, only a small island shows up close to zero frequency for small fields, similarly to d-wave superconductors³³.

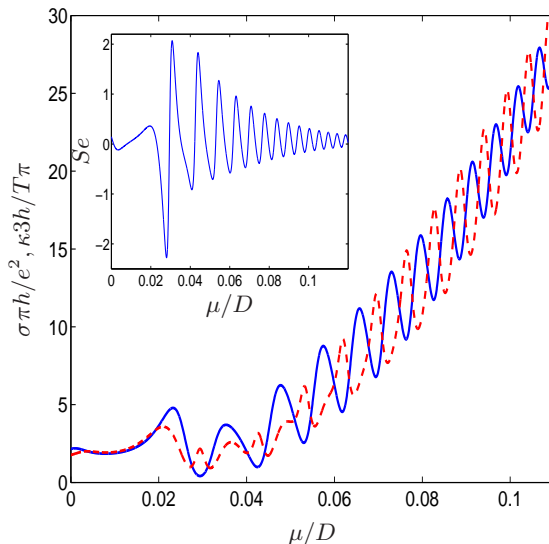


FIG. 5: The electric (blue solid line) and heat (red dashed line) conductivity and the Seebeck coefficient (inset) are shown as a function of the chemical potential for $T = 0.001D$, $N = 1000$, $n_i = 0.001$. Due to the antiphase oscillations, the Wiedemann-Franz law is violated.

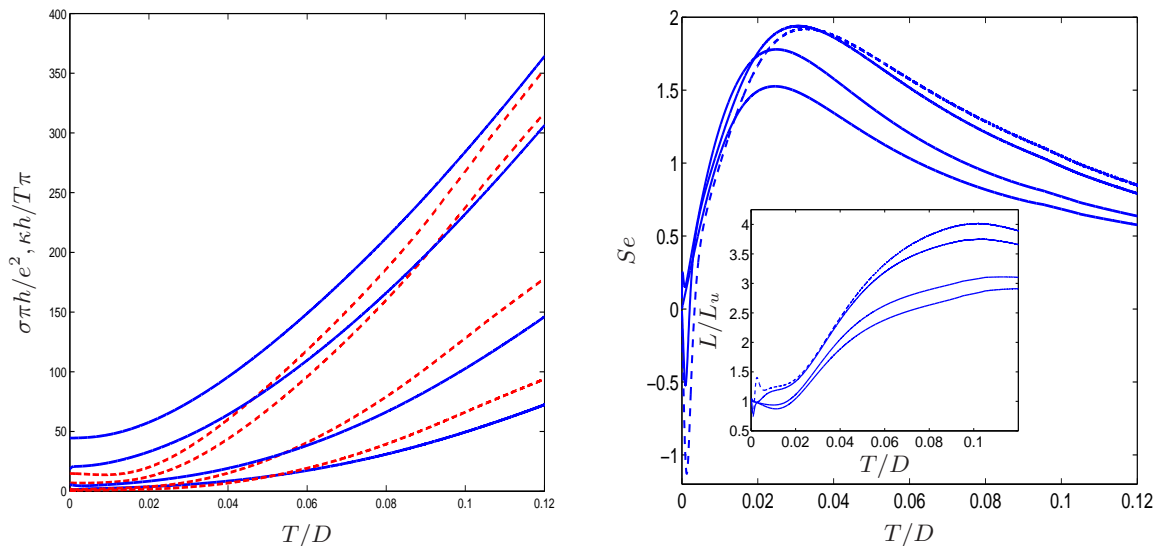


FIG. 6: (Color online) The electric (blue solid line) and heat (red dashed line) conductivity are shown in the right panel for $n_i=0.001$, $\mu = 0.05D$, $N=600, 1000, 3000$ and 10000 from bottom to top. Note the $1/\pi^2$ reduction of the heat conductivity. The right panel shows the Seebeck coefficient and the Lorentz number (inset) for the same parameters from top to bottom, with dashed line for $N = 600$. Note the violation of the Wiedemann-Franz law at low temperatures at high fields (smaller N)!

By increasing the field, oscillations become visible, corresponding to Landau levels. By further increasing the field, these become separated from each other, and clean gaps appear between the levels, in which intragap states, small islands show up at high field. The non-Lorentzian broadening of Landau levels and the intragap features differ from previous studies assuming a constant scattering rate, and should be detected experimentally in graphene.

Both the electric and thermal conductance shows Shubnikov-de Haas oscillation in magnetic field, which disappear for small fields and higher temperatures. These are periodic in $1/B$, similarly to normal metals, in spite of the different Landau quantization. The Seebeck coefficient shares these features, but its oscillations are really large as opposed to σ and κ . The Wiedemann-Franz law stays close to unity, except at certain fields, where large deviations are encountered, which vanish with decreasing field. Besides oscillations, both σ and κ decreases with field, since the larger the cyclotron frequency, the smaller the probability of finding states around μ . These are in agreement with experiments on the thermal conductivity of highly oriented pyrolytic graphite^{7,8}. Oscillations are also present as a function of chemical potential, similarly to experimental findings³.

The temperature dependence of the conductivities is rather conventional, both σ and κ increases with temperature steadily, regardless to the value of the chemical potential. The Seebeck coefficient exhibits a broad bump around $T \sim \mu$, and decreases afterwards. The Wiedemann-Franz law is obeyed for small temperatures and field, but violated for higher values.

Acknowledgments

This work was supported by the Hungarian Scientific Research Fund under grant number OTKA TS049881.

-
- * Electronic address: dora@kapica.phy.bme.hu
- ¹ C. Berger, Z. M. Song, T. B. Li, X. B. Li, A. Y. Ogbazghi, R. Feng, Z. T. Dai, A. N. Marchenkov, E. H. Conrad, and P. N. First, *J. Phys. Chem. B* **108**, 19912 (2004).
 - ² K. S. Novoselov, A. K. Geim, S. V. Morozov, D. Jiang, Y. Zhang, S. V. Dubonos, I. V. Grigorieva, and A. A. Firsov, *Science* **306**, 666 (2004).
 - ³ K. S. Novoselov, D. Jiang, F. Schedin, T. J. Booth, V. V. Khotkevich, S. V. Morozov, and A. K. Geim, *Proc. Natl. Acad. Sci. U.S.A.* **102**, 10451 (2005).
 - ⁴ A. Bostwick, T. Ohta, T. Seyller, K. Horn, and E. Rotenberg, *Nature Physics* **3**, 36 (2007).
 - ⁵ S. Y. Zhou, G.-H. Gweon, J. Graf, A. V. Fedorov, C. D. Spataru, R. D. Diehl, Y. Kopelevich, D.-H. Lee, S. G. Louie, and A. Lanzara, *Nature Physics* **2**, 595 (2006).
 - ⁶ K. S. Novoselov, A. K. Geim, S. V. Morozov, D. Jiang, M. I. Katsnelson, I. V. Grigorieva, S. V. Dubonos, and A. A. Firsov, *Nature* **438**, 197 (2005).
 - ⁷ R. Ocana, P. Esquinazi, H. Kempa, J. H. S. Torres, and Y. Kopelevich, *Phys. Rev. B* **68**, 165408 (2003).
 - ⁸ K. Ulrich and P. Esquinazi, *J. Low Temp. Phys.* **137**, 217 (2004).
 - ⁹ A. A. Nersesyan and G. E. Vachnadze, *J. Low T. Phys.* **77**, 293 (1989).
 - ¹⁰ A. A. Nersesyan, G. I. Japaridze, and I. G. Kimeridze, *J. Phys. Cond. Mat.* **3**, 3353 (1991).
 - ¹¹ S. Chakravarty, R. B. Laughlin, D. K. Morr, and C. Nayak, *Phys. Rev. B* **63**, 094503 (2001).
 - ¹² H. Ikeda and Y. Ohashi, *Phys. Rev. Lett.* **81**, 3723 (1998).
 - ¹³ A. Virosztek, K. Maki, and B. Dóra, *Int. J. Mod. Phys. B* **16**, 1667 (2002).
 - ¹⁴ K. Behnia, R. Bel, Y. Kasahara, Y. Nakajima, H. Jin, H. Aubin, K. Izawa, Y. Matsuda, J. Flouquet, Y. O. Y. Haga, et al., *Phys. Rev. Lett.* **94**, 156405 (2005).
 - ¹⁵ R. Bel, H. Jin, K. Behnia, J. Flouquet, and P. Lejay, *Phys. Rev. B* **70**, 220501 (2004).
 - ¹⁶ S. G. Sharapov, V. P. Gusynin, and H. Beck, *Phys. Rev. B* **67**, 144509 (2003).
 - ¹⁷ S. G. Sharapov, V. P. Gusynin, and H. Beck, *Phys. Rev. B* **69**, 075104 (2004).
 - ¹⁸ V. P. Gusynin and S. G. Sharapov, *Phys. Rev. B* **71**, 125124 (2005).
 - ¹⁹ V. P. Gusynin and S. G. Sharapov, *Phys. Rev. Lett.* **95**, 146801 (2005).
 - ²⁰ V. P. Gusynin and S. G. Sharapov, *Phys. Rev. B* **73**, 245411 (2006).
 - ²¹ V. P. Gusynin, S. G. Sharapov, and J. P. Carbotte, *Phys. Rev. Lett.* **96**, 256802 (2006).
 - ²² V. P. Gusynin, V. A. Miransky, S. G. Sharapov, and I. A. Shovkovy, *Phys. Rev. B* **74**, 195429 (2006).
 - ²³ A. A. Abrikosov, L. P. Gor'kov, and I. E. Dzyaloshinski, *Methods of Quantum Field Theory in Statistical Physics* (Dover Publications, New York, 1963).
 - ²⁴ N. M. R. Peres, A. H. C. Neto, and F. Guinea, *Phys. Rev. B* **73**, 241403 (2006).
 - ²⁵ N. M. R. Peres, F. Guinea, and A. H. Castro-Nero, *Phys. Rev. B* **73**, 125411 (2006).
 - ²⁶ N. H. Shon and T. Ando, *J. Phys. Soc. Jpn.* **67**, 2421 (1998).
 - ²⁷ T. Ando, Y. Zheng, and H. Suzuura, *J. Phys. Soc. Jpn.* **71**, 1318 (2002).
 - ²⁸ A. A. Abrikosov, *Fundamentals of the Theory of Metals* (North-Holland, Amsterdam, 1998).
 - ²⁹ G. W. Semenoff, *Phys. Rev. Lett.* **53**, 2449 (1984).
 - ³⁰ J. Gonzalez, F. Guinea, and M. A. H. Vozmediano, *Nucl. Phys. B* **406**, 771 (1993).
 - ³¹ G. D. Mahan, *Many particle physics* (Plenum Publishers, New York, 1990).
 - ³² M. Jonson and G. D. Mahan, *Phys. Rev. B* **21**, 4223 (1980).
 - ³³ Y. Sun and K. Maki, *Phys. Rev. B* **51**, 6059 (1995).
 - ³⁴ T. Hotta, *Phys. Rev. B* **52**, 13041 (1995).
 - ³⁵ M. Jonson and S. M. Girvin, *Phys. Rev. B* **29**, 1939 (1984).
 - ³⁶ H. Oji and P. Streda, *Phys. Rev. B* **31**, 7291 (1985).